Journal of Power Sources 220 (2012) 42–46

Contents lists available at SciVerse ScienceDirect

Journal of Power Sources

journal homepage: www.elsevier.com/locate/jpowsour

Short communication

Study on surface topography of 446M stainless steel as a bipolar plate on interfacial contact resistance of polymer electrolyte membrane fuel cell

Kwang Min Kim [a,*], Seok Nyeon Kim [a], Jong Hee Kim [b], Yun Yong Lee [b], Kyoo Young Kim [a]

[a] Graduate Institute of Ferrous Technology, Pohang University of Science and Technology, San 31, Hyoja-Dong, Pohang 790-784, Republic of Korea
[b] POSCO Technical Research Laboratories, Pohang 790-785, Republic of Korea

HIGHLIGHTS

- The roughness of bipolar plate can affect deformation of the carbon fibers in GDL.
- The higher deformation of carbon fibers leads to larger real contact area.
- The rough stainless steel has a lower ICR value than the fine one.
- The roughness of bipolar plate can be one of the key factors to decrease ICR.

ARTICLE INFO

Article history:
Received 30 March 2012
Received in revised form
9 July 2012
Accepted 31 July 2012
Available online 8 August 2012

Keywords:
Stainless steel bipolar plate
Polymer electrolyte membrane fuel cell
Interfacial contact resistance
Surface roughness
Finite element method

ABSTRACT

The effect of the surface topography of 446M ferritic stainless steel as a bipolar plate for polymer electrolyte membrane fuel cell (PEMFC) is evaluated by interfacial contact resistance (ICR) measurement and finite element method (FEM) simulation. When the surface of stainless steel is in contact with the carbon paper under load, the surface roughness of stainless steel can affect the degree of deformation of the carbon fiber. Moreover, the higher deformation of carbon fiber under load in the rougher stainless steel could lead to larger real contact area between stainless steel and carbon fiber, and consequently the rough one has a lower ICR value than the fine one. The results suggest that the topography of stainless steel as a bipolar plate significantly affects the ICR. Furthermore, it was found that topography of bipolar plate is one of the key factors to decrease ICR.

1. Introduction

The development of a proper metallic bipolar plate material for polymer electrolyte membrane fuel cell (PEMFC) is one of the key issues for the successful commercialization of PEMFC. Among the candidate metallic materials, stainless steel has been extensively studied because it has a high mechanical strength, high chemical stability, low gas permeability, and low production cost [1–3]. The major concerns for stainless steel bipolar plate have been corrosion and interfacial contact resistance (ICR) of the bipolar material [1]. Particularly, most of the recent research on stainless steels is related to decreasing the ICR by way of coatings [4–6], and nitridation [7,8] because the ICR of bare stainless steels is too high to apply for the bipolar plate material. However, it has been shown that such additional coatings are not beneficial for long-term operation of PEMFC [1,9].

ICR is affected by a number of parameters, such as the bulk and coating material property, surface topology, composition and structure of passive film, assembly pressure and operational condition [10]. However, there has been little study on the effect of surface topology on ICR. Since ICR mainly develops at the interface between the bipolar plate and electrode backing [2], it is necessary to investigate the effect of surface roughness on ICR in relation to the mechanical property and morphology of the electrode backing for which carbon paper is widely used as the gas diffusion layer (GDL).

In this study, the effect of the surface topography of 446M ferritic stainless steel on ICR is examined by ICR measurement and finite element method (FEM) simulation. FEM simulation focuses on the real contact area between the stainless steel and GDL to verify the effect of surface topography on ICR.

* Corresponding author. Tel.: +82 54 279 9237; fax: +82 54 279 9299.
E-mail address: bbaga@postech.ac.kr (K.M. Kim).

0378-7753/$ – see front matter © 2012 Elsevier B.V. All rights reserved.
http://dx.doi.org/10.1016/j.jpowsour.2012.07.102

2. Experimental

2.1. Materials

The specimen used in this study was 446M ferritic stainless steel. The chemical composition of 446M is given in Table 1. After hot rolling to 4 mm, the specimen was homogenized at 1080 °C for 10 min, followed by water cooling. The plates were cut into the specimens with 1.5 cm diameter. Mechanical polishing was used to control the surface roughness of specimens. The surface roughness of specimens was controlled by polishing them with various kinds of SiC abrasive papers (40, 60, 100, 400, 600, 1200 grit). After mechanical polishing, the surface profile was scanned to measure the average roughness (R_a) using a profilometer VEECO Dektak 150 at a scan rate of 25 μm s^{-1} over 5 mm length.

The morphology of the specimens was analyzed using Hitachi SU-6600 scanning electron microscopy (SEM) after mechanical polishing.

2.2. Interfacial contact resistance (ICR)

The method for ICR measurement has been previously described [11]. In short, the ICR of specimens was evaluated by measuring the potential value when a current density in the range of −80 mA cm^{-2}–80 mA cm^{-2} was continuously applied to two copper end plates. The resistance of end plates (Cu) and interfacial resistance ($R_{Cu/S}$) between the Cu end plates and specimen can be ignored in this measurement since total resistance was determined by voltage measurement between the two stainless steel specimens. Therefore, the total measured resistance was a sum of the two interfacial components ($2 \cdot R_{P/C}$) between the passive film and carbon paper. However, the resistance of carbon paper (R_C) was ignored since its value was negligible. The ICR value in this study was calculated simply by dividing the measured total resistance by two. The compression force was applied from 60 N cm^{-2} to 210 N cm^{-2} at intervals of 30 N cm^{-2} to simulate PEMFC stacking condition.

3. Finite element (FE) analysis

FE analysis was carried out to verify the relationship between the specimen roughness and real contact area during a compression test of carbon paper as GDL on the specimen. To explicitly confirm the effect of roughness, the specimen polishing conditions with #40 and #1200 were applied for FE-analysis. FE-simulations were conducted with the commercial FE program, ABAQUS. Since the contact area is strongly sensitive to the size of elements in the contact surface, the density of the element in the vicinity of the surface should be enormously elevated for accurate simulation result. Accordingly, the total computation time also increases proportional to the number of the elements. Therefore, a dynamic explicit FE method for a solver was recommended for computational efficiency. Details will be explained in the ensuing sections. Finally, the real contact area with respect to the reaction force of specimen will be calculated by ABAQUS program.

3.1. Description of contact between GDL and stainless steel

To understand the effect of roughness related to the contact area, the FE simulations of the compression test need to be performed with different level of surface roughness, R_a. In the microscale, the GDL can be treated as an aggregation of the carbon fibers because the approximated height of the fiber is in the order of several μm. Therefore, the verification should be performed with respect to the interaction between the single carbon fiber and surface of the stainless steel specimen in microscale.

The surface of the stainless steel specimen shows textured roughness in the direction of polishing as shown in Fig. 1(a). However, the carbon fibers in the GDL are organized in randomly oriented directions, which can be seen in Fig. 1(b). To make the problem simple, the orientation of the fiber was assumed to be perpendicular to the surface texture of the specimen, as shown in Fig. 2(a), and the deformation was constrained in the 2-dimensional space corresponding to the transverse section of the fiber, as illustrated in Fig. 2(b). To ignore the effect of geometric position between the fiber and the specimen, the length of the fiber was assumed infinite. Furthermore, the surface pattern of the specimen is simplified as a sinusoidal curve which has a circular curvature of radius, R, estimated with the roughness of each specimen. In 2-dimensional space, the carbon fiber is simply assumed to be a rectangular shape with 10 μm in height. The thickness of the simplified carbon fiber is assumed to be unity. Using the pattern of the specimen and the infinite length of the fiber, periodicity can be determined, which is computationally effective. Since the yield strength of the specimen (STS 446M) is extremely larger than that of the carbon fiber (SGL-10-BA), the stainless steel specimen can be defined as a rigid body, meaning an un-deformable solid. These assumptions will be applied to the configuration of the simulation by using the pre-processor, ABAQUS/CAE.

3.2. FEM model

The carbon fiber is modeled with a 2D plane strain element with reduced integration, CPE4R and the thickness is set as unity. Considering the circular curvature of the specimen surface, R, the unit length of the carbon fiber in contact with specimen can be defined. Using the periodicity of the given geometry, one period of the total surface length can be defined as a representative window for the FE simulation. Therefore, the length of the fiber is defined as one period of surface pattern, λ as shown in Fig. 2(b). Fig. 3 shows that the relationship between the R value and R_a of specimen assumed as a sinusoidal curve which has a circular curvature of radius, R. In Fig. 3(a), red line (in web version) indicates 2D surface of specimen assumed as a sinusoidal curve with a circular curvature of radius, R. According to the definition of R_a, the area of the shaded part in Fig. 3(a) should be equal to that in Fig. 3(b). From this relationship between R and R_a value of the specimen, the magnitude of R can be calculated from the measured R_a value of the specimens polished with #40 and #1200, with an assumption that the surface profile has a perfect sinusoidal configuration. The calculated values are listed in Table 2. The R value of the specimen polished with #40 is almost 87.6 times larger than that of the specimen polished with #1200. Furthermore, the carbon fiber is assumed to be a hyper-elastic material and its stress–strain curves, measured by the biaxial compression tests, are referred to in the literature by Iwao Nitta et al. [12]. In addition, the volumetric response during deformation is described by the Poisson's ratio of

Table 1
Chemical composition of experimental stainless steel alloys (unit: wt.%).

Specimen	C	Si	Mn	P	S	Cr	Ni	Cu	Ti	Mo	Fe
446M	<0.004	<1.00	<1.50	<0.005	<0.005	26.63	0.183	<0.50	<0.06	2.04	Bal.

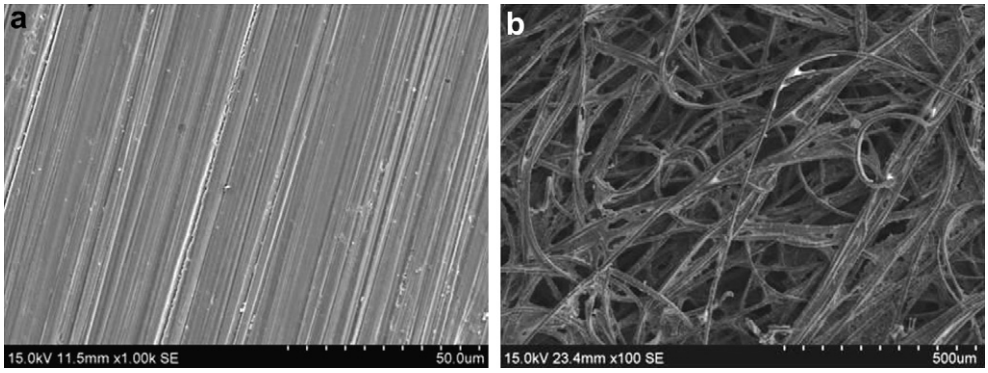

Fig. 1. SEM images of (a) polished surface on specimen and (b) carbon paper.

0.475 and the density of the fiber is assumed to be 2.2×10^{-7} g cm^{-3}.

To simulate a quasi-static problem with a dynamic explicit FE program, the mass scaling technique is necessary and optimized value is used, which results in negligible kinetic energy, or dynamic effect. In terms of the friction between the carbon fiber and specimen surface, the friction is ignored because a negligible magnitude of friction coefficient is reported in the literature [13].

Once the simulation finishes, the contact area can be calculated in the post-processing stage. To increase accuracy in the calculation of the contact area, the elements near the contact surface need to be as dense as possible. Considering the current computation capacity and computational cost, an appropriate number of elements are selected on the surface and one particular example.

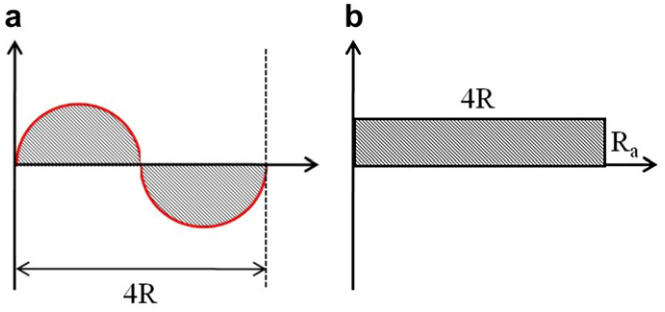

Fig. 3. The relationship between the R value and R_a of specimen. (a) 2D surface of specimen assumed as a sinusoidal curve with a circular curvature of radius, R; and (b) the area according to the definition of R_a.

4. Results and discussion

Abrasive paper polishing was performed to investigate the effect of surface roughness of a stainless steel bipolar plate on ICR. Table 3 lists the result of the average roughness measurement of 446M using the profilometer after polishing with various kinds of abrasive papers. Table 3 indicates that the surface roughness increases with decreasing abrasive paper grit.

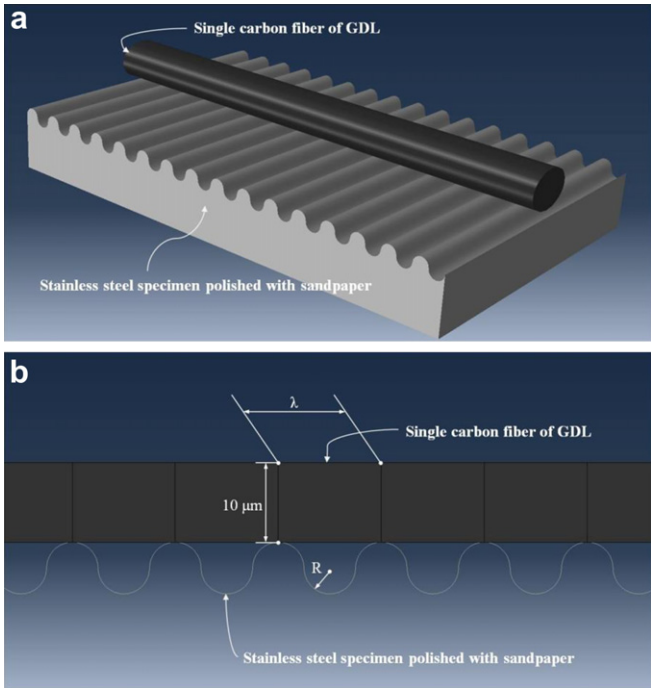

Fig. 2. (a) 3D description of the single carbon fiber of the GDL and the stainless steel specimen surface in microscale, (b) 2D description of the single carbon fiber of the GDL and stainless steel specimen surface in microscale (λ: period, R: curvature of the specimen surface).

Fig. 4 shows the ICR test results for 446M after polishing with various abrasive papers. From Fig. 4, it is noted that ICR for all the specimens decreases with increasing the compaction pressure regardless of roughness of specimens. It is because the contact area or the number of spots increases with deformation of carbon paper under elevated pressure [14]. Furthermore, Fig. 4 indicates that 446M with a rougher surface shows a lower ICR value than that with a finer surface. 446M polished with #40 has the roughest surface and shows the lowest ICR value among all the tested specimens. This can be explained by a change of the real contact area between the stainless steel surface and carbon paper, depending on the surface roughness of the stainless steel. It suggests that the real contact area of a rough surface with a lower ICR is larger than that of a fine surface with a higher ICR value.

Fig. 5(a) shows FE analysis results of the real contact area between stainless steel and carbon paper. In FE analysis, stainless steel is considered as rigid material, meaning an un-deformed solid because its elastic modulus and yield strength values are far higher than the values of carbon paper [14]. Therefore, when

Table 2
The curvature of the specimen surface and the period of the fiber calculated with the measured R_a.

Specimens	R_a (μm)	R (μm)	λ (μm)
#40	2.547	3.243	12.972
#1200	0.029	0.037	0.148

Table 3
Average roughness (R_a) of 446M polished with various grit size abrasive papers.

Abrasive paper grit size	Average roughness, R_a(μm)
40	2.547
60	1.906
100	0.446
400	0.129
600	0.042
1200	0.029

stainless steel contacts with carbon paper, carbon fiber should be only deformed under the load and degree of deformation on carbon fiber is important for real contact area and change of real contact area between specimen surfaces. In Fig. 5(a), the real contact area of rough 446M polished with # 40 is larger than that of fine 446M polished with # 1200. Fig. 5(b) shows that deformed shape of carbon fiber on fine and rough surface 446M under the load. The carbon fiber and 446M shown in Fig. 5(b-I and b-II) are plotted with the same magnification, and the inset in Fig. 5(b-I) is the enlarged view of the interface between carbon fiber and 446M for easy comparison. In the fine 446M, deformation of carbon fiber is relatively dispersed, as compared with rough 446M under the load, because the fine specimen has more contact points between carbon paper and the specimen than the rough one at initial contact. Accordingly, carbon fiber on rough 446M is more deformed than that on fine one under load. As mentioned above, because specimen is considered as un-deformed material, the change of real contact area between specimen and carbon fiber depends on the degree of deformation on carbon fiber. In the rough 446M, therefore, the higher deformation of carbon fiber under load as shown in Fig. 5(b) could lead to larger real contact area between specimen and carbon fiber and finally rough 446M has a lower ICR value than fine one. These results indicate that the roughness of stainless steel affects the ICR value significantly and the ICR value of 446M can be decreased to an optimum value by proper control of its surface roughness. In order to further improve the electrical conductivity, a systematic investigation on the effect of surface roughness on ICR is required in the future, using experiments controlling the surface roughness by various methods including mechanical polishing and chemical surface treatment.

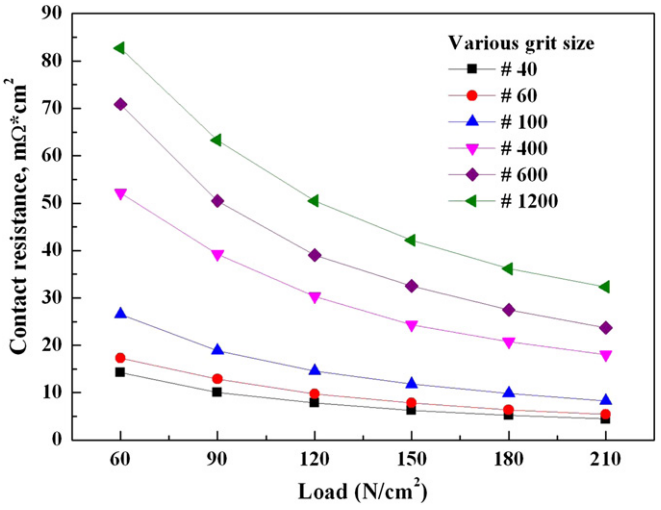

Fig. 4. Interfacial contact resistance for 446M which was polished with various abrasive papers.

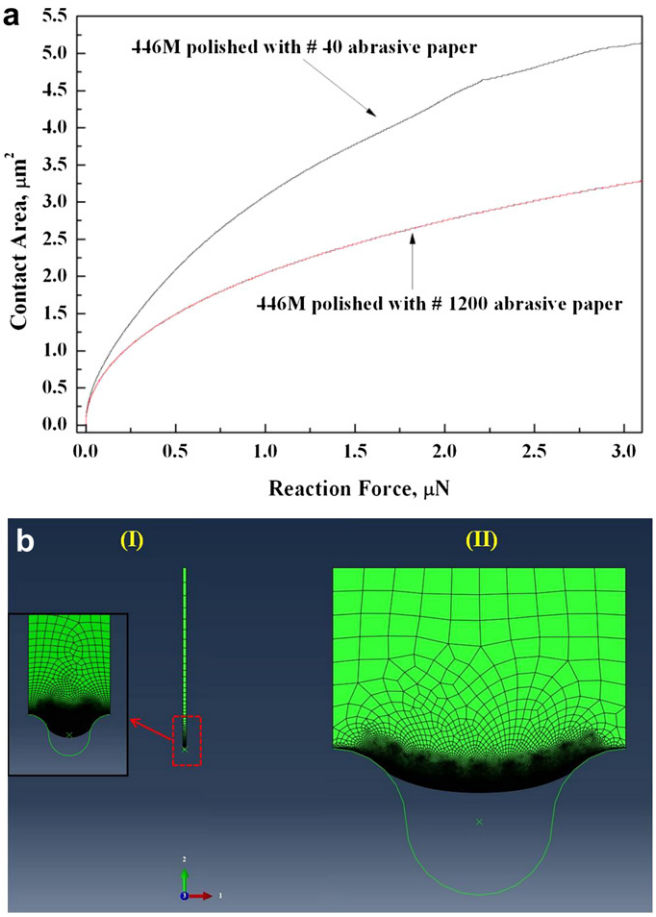

Fig. 5. (a) FE analysis results of the real contact area between stainless steel and carbon paper for 446M after polishing with # 40 and # 1200, (b) deformed shape of carbon fiber on 446M which was polished with (I) # 1200 and (II) # 40. Inset in (I) is the enlargement of the deformed shape of carbon fiber.

5. Conclusions

Ferritic stainless steel type 446M as a bipolar plate for PEMFC was investigated to understand the effect of the surface topography on ICR by measurement of ICR and FEM simulation. In ICR measurement and FE analysis, 446M with a rougher surface shows a lower ICR value than the one with a finer surface and the real contact area of the former is larger than that of the latter. The roughness of stainless steel affects significantly the ICR value because of the real contact area between the stainless steel and the gas diffusion layer under loading conditions. Therefore, in order to further improve the electrical conductivity of the bipolar plate, a further study is required to control the surface roughness by various methods for commercial application.

Acknowledgments

This investigation was supported by a POSCO grant.

References

[1] A. Hermann, T. Chaudhuri, P. Spagnol, Int. J. Hydrogen Energy 30 (2005) 1297.
[2] H. Wang, J.A. Turner, J. Power Sources 128 (2004) 193.
[3] R.C. Makkus, A.H.H. Janssen, F.A. Bruijn, R.K.A.M. Mallant, J. Power Sources 86 (2000) 274.
[4] H. Wang, J.A. Turner, J. Power Sources 170 (2007) 387.
[5] H. Wang, J.A. Turner, X. Li, G. Teeter, J. Power Sources 178 (2008) 238.
[6] Y. Wang, D.O. Northwood, Int. J. Hydrogen Energy 32 (2007) 895.

[7] K.H. Lee, S.H. Lee, J.H. Kim, Y.Y. Lee, Y.H. Kim, M.C. Kim, et al., Int. J. Hydrogen Energy 34 (2009) 1515.
[8] H. Wang, M.P. Brady, G. Teeter, J.A. Turner, J. Power Sources 138 (2004) 86.
[9] H. Tawfik, Y. Hung, D. Mahajan, J. Power Sources 163 (2007) 755.
[10] Y. Zhou, G. Lin, A.J. Shin, S.J. Hu, J. Power Sources 163 (2007) 777.
[11] K.M. Kim, J.H. Park, J.H. Kim, K.Y. Kim, Int. J. Hydrogen Energy 36 (2011) 9926.
[12] I. Nitta, O. Himanen, M. Mikkola, Fuel Cells 8 (2008) 111.
[13] K. Jradi, M. Schmitt, S. Bistac, Appl. Surf. Sci. 255 (2009) 4219.
[14] A. Kraytsberg, M. Auinat, Y. Ein-Eli, J. Power Sources 164 (2007) 697.